Characteristics of Dielectric Holograms*

Abstract: The diffraction efficiency and signal-to-noise ratio for two-dimensional and volume diffuse-signal-beam holograms are calculated and experimentally determined. Calculations are based on the statistical properties of the signal beam, and exact integrals rather than series approximations are used. High signal-to-noise ratio and high diffraction efficiency are possible, with the peak calculated diffraction efficiency being 22% for two-dimensional and 64% for volume holograms. The experimentally achieved efficiencies were 12% for two-dimensional and 36% for volume holograms.

Introduction

The possibility of converting a hologram intensity pattern into phase variations was recognized by Rogers¹ soon after the invention of holography. More recently, numerous papers have dealt with theoretical and experimental aspects of two-dimensional phase holograms.²⁻¹⁵ Most of the published theoretical work has been concerned with diffraction efficiencies achieved by the recorded interference pattern of two plane wavefronts of uniform amplitude. 7,11 Cathey determined conditions for which phase holograms have a constant ratio of signal-wave to reconstructed-wave amplitude, and a similar estimate was made by Urbach and Meier.4,5 In this paper we calculate the average diffraction efficiency of a diffusesignal-beam dielectric two-dimensional hologram and the signal-to-noise ratio of the reconstructed wavefront. In these calculations we assume that refractive index change within the emulsion is proportional to the exposure, and we consider only the noise generated by the intermodulation terms.

The experimentally achieved diffraction efficiencies and signal-to-noise ratios of diffuse-signal-beam dielectric volume holograms have been previously reported. ^{16–19} Theoretical calculations have been made independently by Baugh²⁰ and by the authors. ²¹ The results do not agree, apparently because different approximations were used. We include here a summary of the calculations for diffraction efficiency and signal-to-noise of dielectric volume holograms as derived by the authors.

Recording of diffuse wavefronts in dielectric media

To calculate diffraction efficiencies and signal-to-noise ratios of the reconstructed wavefronts we shall first specify the wavefronts incident upon the hologram. Let the reference wave be $s_0 = a_0 \exp j\phi_0$ and the signal wavefront be $s = a_s \exp j\phi_s$, where only a_0 is assumed to be a constant. The irradiance I of the hologram is then

$$I = |s_0 + s|^2$$

$$= a_0^2 + a_s^2 + 2a_0a_s \cos \phi_{0s}, \qquad (1)$$

where $\phi_{0s} = \phi_s - \phi_0$. For the case in which the hologram is recorded in a two-dimensional medium, a_s and ϕ_{0s} are variables of the hologram surface coordinates only; for three-dimensional recording media, we assume that a_s is still only a function of the surface coordinates, but that ϕ_{0s} is a function of the medium's volume coordinates. The latter specification is quite reasonable since we can have a high spatial carrier frequency and a narrow signal beam (or angle subtended by the object at the hologram).

We shall assume that the incident signal wavefront has the Rayleigh-probability amplitude distribution

$$p(a_s) = (a_s/\sigma^2) \exp(-a_s^2/2\sigma^2),$$
 (2)

where σ^2 is the variance of the signal defined as $2\sigma^2 = \langle a_{\rm s}^2 \rangle$. This probability distribution arises from the summation of the amplitudes of a large number of radiators, ²² the phases of which are equally likely to have any value between 0 and 2π . An irregular or diffuse surface that reflects or transmits an incident wavefront can be considered to have these properties.

The authors are with the Radar and Optics Laboratory of the Institute of Science and Technology at the University of Michigan, Ann Arbor, Michigan

⁴⁸¹⁰⁷This work was supported by the United States Air Force Avionics Laboratory, Wright-Patterson Air Force Base, Ohio under Contracts F33615-67-C-1814 and F33615-68-C-1310.

We can now define the beam ratio K as

$$K = a_0^2 / \langle a_s^2 \rangle. \tag{3}$$

The variance σ^2 can then be expressed as

$$\sigma^2 = a_0^2 / 2K. \tag{4}$$

Because we are dealing with dielectric holograms, we assume that the exposure is converted into a corresponding refractive-index variation and that the refractive-index change is proportional to exposure; i.e.,

$$\Delta n = m\tau I,\tag{5}$$

where m is the slope of exposure versus refractive-index change and τ is the exposure time. The assumption of linear refractive-index change as a function of exposure is probably not realistic for bleached photographic emulsions, but other recording media show this characteristic. Other authors have also used this assumption. ^{7,20}

Phase modulation of incident wavefronts can also be achieved by converting exposure into a corresponding emulsion relief pattern. This technique has been frequently used, (Refs. 2, 3, 9, 10, 12, 13) but we do not consider it here because the relief pattern is highly sensitive to the spatial frequency, and this characteristic would greatly complicate the calculations.

From Eqs. (1) and (5) we obtain the refractive-index change Δn due to exposure by the incident wavefronts:

$$\Delta n = m\tau a_0^2 + m\tau a_s^2 + 2m\tau a_0 a_s \cos \phi_{0s}$$

= $\Delta n_0 + \Delta n_N + \Delta n_s$, (6)

where $\Delta n_0 = m\tau a_0^2$, $\Delta n_{\rm N} = m\tau a_{\rm s}^2$ and $\Delta n_{\rm s} = 2m\tau a_0 a_{\rm s}$ cos ϕ_{0s} . For the two-dimensional case, the phase delay $\Delta\Psi$ caused by refractive-index variations in the recording medium is given by

$$\Delta\Psi = (2\pi d/\lambda \cos \theta)\Delta n,\tag{7}$$

where λ is the wavelength of light, d the thickness of the recording medium, and θ the angle between the normal to the surface and the direction of the incident wavefront within the medium.

The transmittance T of the hologram can be expressed as $T=e^{i\Delta\Psi}$. From Eqs. (6) and (7) and the above expression it is evident that the terms of Eq. (6) become products in the expression $T=e^{i\Delta\Psi}$. The first term of Eq. (6) is a constant and will be neglected. The second term is a random refractive-index change, and the third causes reconstruction of the recorded wavefront. We shall calculate the diffraction efficiency from the third term and the degradation of the reconstructed wavefront from the second term of Eq. (6).

For the volume recording of the signal term, Δn_s will be used directly in the expression for diffraction efficiency, as will be shown later.

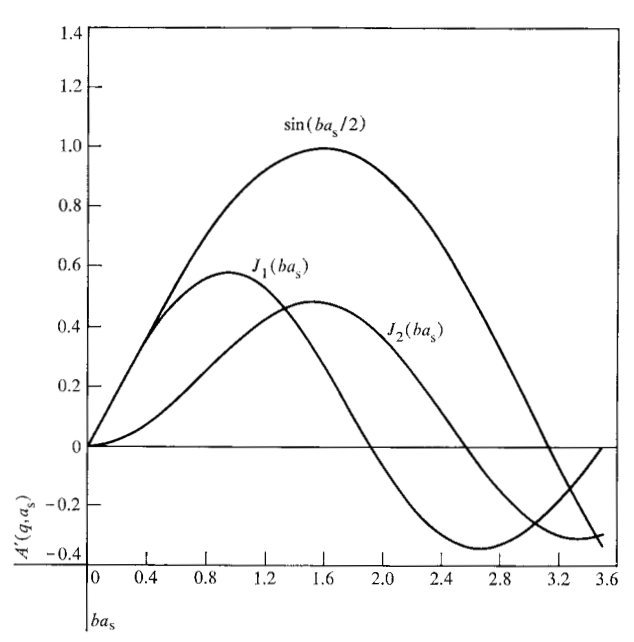


Figure 1 Response of dielectrically modulated holograms. The reconstructed wave amplitude, normalized with respect to the incident wave amplitude, is given by $A'(q, a_s) = J_q(ba_s)$ for two-dimensional holograms and $A'(q = 1, a_s) = \sin(\frac{1}{2}ba_s)$ for volume holograms.

Two-dimensional recording media

• Properties of diffracted orders

From Eqs. (6) and (7) we find that the complex transmittance T_s of the medium caused by the third term of Eq. (6) is

$$T_{\rm s} = \exp \left[(j4\pi m\tau \ da_0 a_{\rm s}/\lambda \cos \theta) \cos \phi_{0\rm s} \right]$$

= $\exp \left(jba_{\rm s} \cos \phi_{0\rm s} \right)$, (8)

where $b = 4\pi m\tau da_0/\lambda \cos \theta$. Although the first-order diffracted wavefront is of most interest, the higher-order diffracted wavefronts have some useful properties. To examine these properties let us express Eq. (8) as the infinite series²³:

$$\exp(jba_{s}\cos\phi_{0s}) = \sum_{q=-\infty}^{+\infty} (j)^{q} J_{q}(ba_{s}) \exp(jq\phi_{0s}).$$
 (9)

The right-hand side of Eq. (9) represents a summation of terms each of which reconstructs a wavefront on a different carrier frequency, and these wavefronts are separated from each other.

If we now illuminate the hologram with a wavefront $1 \exp(jq\phi_0)$, and if we neglect the second factor of Eq. (6), then we obtain a reconstructed wavefront of amplitude $A(q, a_s)$ for the q's order:

$$A(q, a_s) = J_q(ba_s) \exp(jq\phi_s). \tag{10}$$

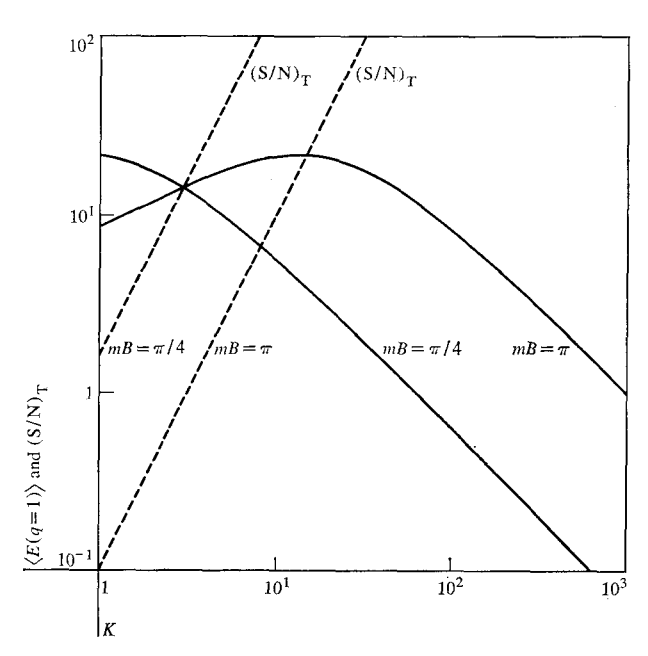


Figure 2 Diffraction efficiency $\langle E(q=1) \rangle$ in percent, and signal-to-noise ratio $(S/N)_T$ of a two-dimensional dielectric hologram versus the reference-to-average signal-beam irradiance K for the first diffracted order.

The phase of the reconstructed wavefront is $q\phi_s$ or is multiplied by the factor q. This characteristic is useful in amplifying phase differences in interferometry. We also note that the first term of the series expansion for a Bessel function, a valid approximation for small values of ba_s , is

$$J_q(ba_s) \approx (b^q/2^q q!)(a_s)^q. \tag{11}$$

Thus, we can obtain an amplification of the wavefront's inherent amplitude variations by using |q| > 1, and for an image-plane hologram, a higher contrast image could be obtained.

Figure 1 shows the response curves for q=1 and q=2. The curve for the first diffracted order shows that response is linear for small values of ba_s as expected from Eq. (11); for the second diffracted order the response is proportional to a_s^2 for small values of ba_s and is linear over a range of higher values of ba_s . All curves show an inverse linearity as ba_s increases further and a 180° phase shift as the response goes through zero. Since such phase reversal generates noise, we consider in our calculations the lower range of ba_s , where phase reversal does not occur.

• Diffraction efficiency

The diffraction efficiency of a two-dimensional phase hologram as a function of q and a_s is simply

$$E(q, a_s) = J_q^2(ba_s). (12)$$

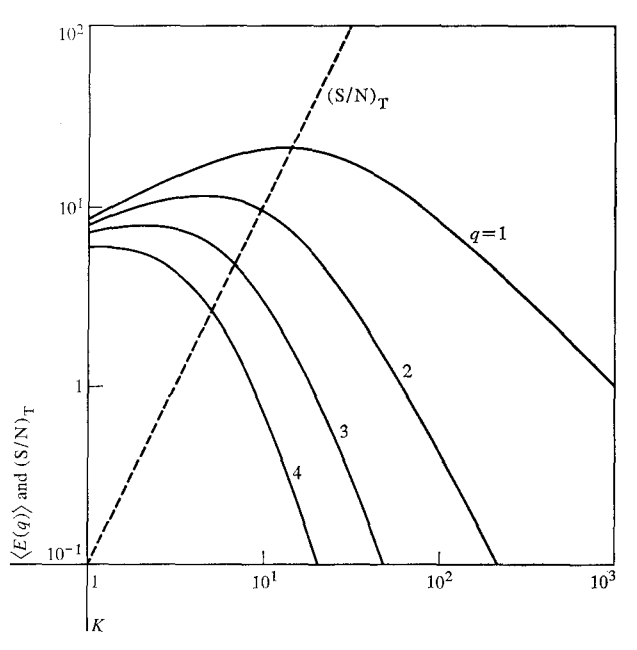


Figure 3 Diffraction efficiency $\langle E(q) \rangle$ in percent, and signal-to-noise ratio $(S/N)_T$ of a two-dimensional dielectric hologram versus the reference-to-average signal-beam irradiance ratio K for the q's diffracted order.

In a typical hologram made of a diffuse object, a_s varies over a wide range of values. Thus we consider the average diffraction efficiency

$$\langle E(q) \rangle = \int_0^\infty p(a_s) J_q^2(ba_s) da_s. \tag{13}$$

Since we assumed that $p(a_s)$ is a Rayleigh probability distribution,

$$\langle E(q) \rangle = \int_0^\infty (a_s/\sigma^2) \exp(-a_s^2/2\sigma^2) J_q^2(ba_s) da_s$$

$$= \exp(-\sigma^2 b^2) I_q(\sigma^2 b^2), \qquad (14)$$

where $I_q(\sigma^2 b^2)$ is a hyperbolic Bessel function of order q. Substituting for σ and b, and letting $B = (2\pi\tau da_0^2)/(\lambda \cos \theta)$, we get

$$\langle E(q) \rangle = \exp(-2m^2B^2/K)I_o(2m^2B^2/K).$$
 (15)

Figure 2 shows the plot of $\langle E(1) \rangle$ for two values of mB; Fig. 3 shows the plot of $\langle E(q) \rangle$ with $mB = \pi$ for several values of q. The maximum efficiency is 22% instead of the 34% for the two-plane-wave case.

In these calculations, we have considered only the third factor of Eq. (6). Since the reconstructed wavefront is multiplied by the second factor of Eq. (6), the intermodulation terms, part of the reconstructed wavefront will be scattered and will create noise in the reconstructed image, which will be calculated next. We may also note

that the various diffracted orders are completely separated from each other and do not create a superposition of images.

• Signal-to-noise ratio in the reconstructed wavefront

The fraction of reconstructed wavefront scattered by the intermodulation terms recorded in two-dimensional media has been previously calculated elsewhere, ²¹ and we include a summary of these calculations here.

Let S be the fraction of light flux not scattered and N=1-S be the fraction of light flux scattered by the intermodulation terms. The phase delay $(\Delta\Psi)_N$ caused by the intermodulation terms is

$$(\Delta \Psi)_{\rm N} = -(2\pi \ d/\lambda \cos \theta)(m\tau a_{\rm s}^2)$$
$$= -(b/2a_0)I_{\rm N}, \tag{16}$$

where $I_N = a_s^2$. We can calculate S by taking the Fourier transform of the phase pattern generated by the second factor of Eq. (6) and evaluating it for the zero spatial-frequency component. Or we can use the equivalent expression for V, where V is the normalized unscattered fraction of light amplitude for a given plane wave generated by the signal term, and $S = VV^*$, where

$$V = \int_0^\infty p(I_N) \exp \left[-j(b/2a_0)I_N\right] dI_N.$$
 (17)

For the Rayleigh-probability amplitude distribution, the corresponding intensity distribution is $p(I_N) = (1/2\sigma^2) \exp(-I_N/2\sigma^2)$. The resulting expression for V is

$$V = [1 + j(b\sigma^2/a_0)]^{-1}.$$
 (18)

After substituting for the constants and using previously mentioned equalities, we find the total reconstructed unscattered-to-scattered flux ratio $(S/N)_T$ to be

$$(S/N)_T = K^2/m^2B^2.$$
 (19)

The quantity $(S/N)_T$ indicates the effect that converting intermodulation terms into a phase pattern has on the ratio of unscattered-to-scattered light flux. $(S/N)_T$ versus K is shown in Fig. 2 for two values of mB. It is evident that by increasing mB and K we can obtain high-diffraction efficiency and high signal-to-noise ratio as well. Scattering or noise caused by granularity of the medium or nonlinearities in the amplitude of the reconstructed wavefront are not included in $(S/N)_T$.

Three-dimensional recording media

The diffraction efficiency from dielectric volume media has also been reported elsewhere, so only a brief summary is given here. As mentioned previously, we consider the case where the interference pattern between the reference and signal beams is recorded as a volume hologram, while the intermodulation terms are recorded as

two-dimensional phase holograms. The signal-to-noise ratio is, therefore, the same as for the two-dimensional case and is given by Eq. (19).

As the basis for calculating the efficiency of diffraction from a volume dielectric hologram, we use the expression for efficiency of diffraction from a recorded two-planewave interference pattern derived by Kogelnik⁷:

$$E(a_s) = \sin^2 \left[(\pi d/\lambda \cos \theta) \Delta n \right], \tag{20}$$

where Δn can be found from Eqs. (5) and (6) and is the same as for two-dimensional media. We find the diffraction efficiency the same way as for two-dimensional media, except that diffraction efficiency as a function of a_n is now given by Eq. (20) instead of Eq. (12):

$$\langle E \rangle = \int_0^\infty (a_s/\sigma^2) \exp(-a_s^2/2\sigma^2) \sin^2(\frac{1}{2}ba_s) da_s$$

= $\frac{1}{2}b^2\sigma^2 \exp(-\frac{1}{2}b^2\sigma^2) {}_1F_1(\frac{1}{2}; \frac{3}{2}; \frac{1}{2}b^2\sigma^2),$ (21)

where ${}_{1}F_{1}(\alpha; v; x)$ is a confluent hypergeometric function, ²⁴

and

$${}_{1}F_{1}(\alpha; v; x) = 1 + \frac{\alpha}{v} x + \frac{\alpha}{v} \left(\frac{\alpha + 1}{v + 1}\right) \frac{x^{2}}{2!} + \frac{\alpha}{v} \left(\frac{\alpha + 1}{v + 1}\right) \left(\frac{\alpha + 2}{v + 2}\right) \frac{x^{3}}{3!} + \cdots$$
 (22)

Substituting for b and σ in Eq. (21), we get $\langle E \rangle = (m^2 B^2 / K)$

$$\cdot \exp(-m^2 B^2 / K)_1 F_1(\frac{1}{2}; \frac{3}{2}; m^2 B^2 / K). \tag{23}$$

Figure 4 shows the diffraction efficiency versus K for several values of mB and also the efficiency of a two-plane-wave interference pattern, as given by Eq. (20). The maximum efficiency for a diffuse signal wave is 64%. It is obvious that higher $(S/N)_T$ is possible with larger constant mB. The results from Eq. (23) and the graphs in Fig. 4 do not apply to the case in which the intermodulation terms are also recorded in volume.

Experimental investigation

Dielectric holograms were made by bleaching developed photographic emulsions. The bleached plates had some residual absorption and, therefore, were not purely dielectric holograms. The average transmittance of these holograms was about 50%, and we can expect the diffraction efficiency also to be lower than the theoretic prediction by about a factor of two.

Several characteristics of the holograms were measured: the diffraction efficiency, signal-to-noise ratio $(S/N)_T$ and contrast ratio $(S/N)_C$ of the image. The object consisted of a square diffuse glass plate with a small opaque rectangle in the center. Contrast was measured at the center

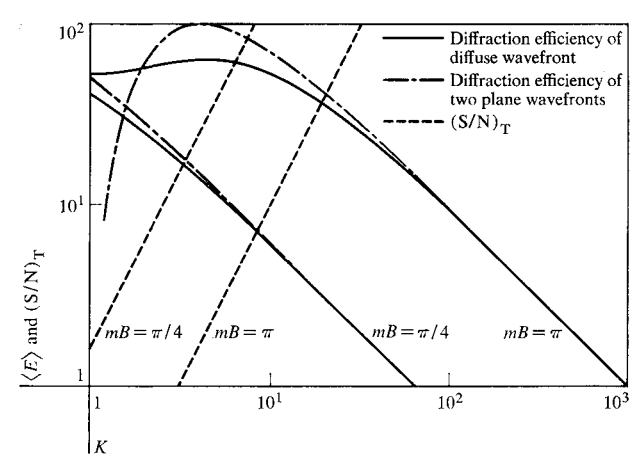
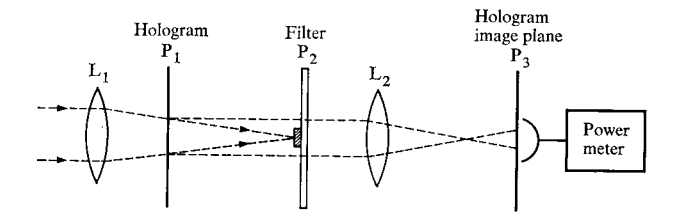


Figure 4 Diffraction efficiency in percent, and signal-to-noise ratio $(S/N)_T$ of a volume dielectric hologram versus the reference-to-average signal-beam irradiance K.

Figure 5 Optical system for measuring (S/N)_T.



of the image. The signal beamwidth, defined as the angle subtended by the object at the hologram plane, was determined by the object-to-hologram distance. For all measurements the emulsion side of the hologram was placed in a liquid gate with xylene to reduce the effects of surface relief patterns.

 $(S/N)_T$ was measured using the optical system shown in Fig. 5. The zero-diffracted order was imaged by lens L_2 onto a power meter at P_3 . With the unscattered portion of light blocked at P_2 , the power reading is proportional to noise N; with all of the zero-diffracted order light falling on the power meter, a reading proportional to S + N is obtained. From these readings $(S/N)_T$ was calculated.

The holograms were recorded on Kodak 649F plates, developed in D-19 for five minutes, rinsed, fixed and washed. They were then bleached as follows:

- 1) 10 minutes in Kodak SH-1 hardener,²⁶
- 2) 10 minutes in CuBr₂ bleach,²⁷
- 3) 4 minutes in Kodak CB6 clearing bath,
- 4) 5 minutes in desensitizing solution.

The plates were rinsed for one minute after the first three steps, but were not washed after the last step. The plates

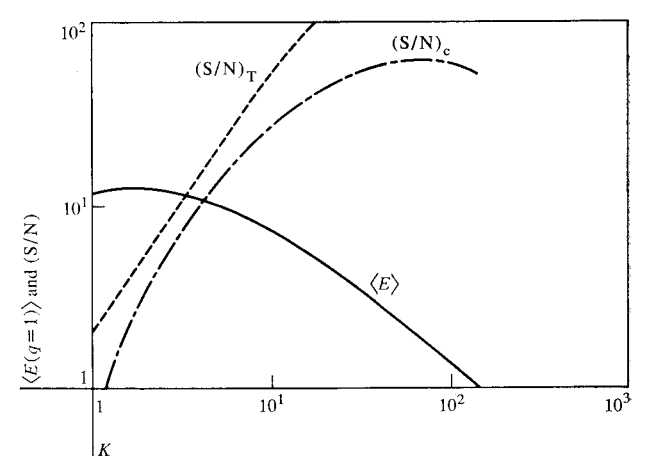


Figure 6 Experimentally measured diffraction efficiency $\langle E(q=1)\rangle$ in percent, for the first diffracted order, signal-to-noise ratio $(S/N)_T$, and contrast ratio $(S/N)_C$ of a two-dimensional dielectric hologram. Test parameters: average density before bleaching 2.6, mean carrier frequency 65 lines/mm, signal beamwidth 0.7°.

were wiped clear of excess water with a windshield wiper blade and then dried in air.

The bleaching solution was the same as described in Ref. 27 except that equal parts of solutions A and B were used without being diluted. The use of hardener eliminated the problems previously encountered with this bleach. The desensitizing solution consisted of 25g of CuBr₂ per liter, with photo flo and Pakasol print-flattening solution added to reduce emulsion shrinkage.

Figure 6 shows the results obtained with a two-dimensional dielectric hologram. A peak efficiency of 12% was reached, about one-half the theoretical maximum. The efficiency was 9% with a corresponding $(S/N)_C = 20$, a good contrast level. The $(S/N)_T$ curve has higher values than $(S/N)_C$, but theoretical considerations indicate $(S/N)_T < (S/N)_C$ for a constant K. This indicates that other sources of noise besides those considered in the calculations are significant. Other possible sources of noise might be grain scattering and lateral distortion of fringe patterns.

Figure 7 shows similar results for a volume hologram. A peak efficiency of 36% was achieved, and 33% efficiency was obtained with $(S/N)_C = 20$. In this case, $(S/N)_T < (S/N)_C$ as expected. The value of $(S/N)_C$ for large K decreases since grain scattering remains constant while the signal level decreases.

Conclusion

Diffraction efficiencies and signal-to-noise ratios were calculated for diffuse-signal-beam holograms recorded in dielectric media. The calculations were based on the assumption of linear refractive-index change as a func-

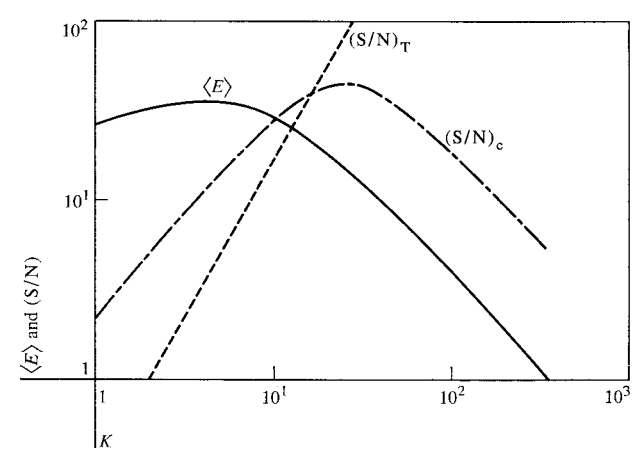


Figure 7 Experimentally measured diffraction efficiency $\langle E \rangle$ in percent, signal-to-noise ratio $(S/N)_T$, and contrast ratio $(S/N)_C$ of a volume dielectric hologram. Test parameters: average density before bleaching 4.0, mean carrier frequency 1330 lines/mm, signal beamwidth 6°.

tion of exposure, Rayleigh-probability amplitude distribution in the signal beam and two-dimensional recording of intermodulation terms. Only noise caused by the conversion of intermodulation terms into a corresponding phase pattern was considered; noise generated by nonlinear transfer characteristics or grain scattering was not included.

Dielectric holograms that depart from the theoretical model in several aspects were experimentally made. The holograms have considerable residual absorption; the emulsion undergoes distortion during processing; the change in exposure versus refractive index is probably not very linear; and grain scattering adds to the noise. Other recording materials have better characteristics.¹⁹

In comparing general trends, agreement can be observed between experimental and theoretical results: $(S/N)_T$ increases with K although, experimentally, at a slower rate than predicted; diffraction efficiency decreases in proportion to K^{-1} at low efficiencies; the shapes of the efficiency curves near the maximum are similar; the differences in maximum efficiencies can be accounted for by the residual absorption of the bleached plates. Closer comparison is difficult since the constants mB are not known for the experimental case.

Dielectric holograms have linear response curves over a range of amplitudes, as shown in Fig. 1. Absorption holograms have similar response curves except that the peak efficiency is approximately 6%. Since, evidently, intermodulation noise can be made negligible in dielectric holograms, images of higher over-all quality should be possible with such holograms.

References

- 1. G. L. Rogers, *Proc. Roy. Soc. Edinburgh* **A63**, 193 (1952)
- 2. W. T. Cathey, Jr., J. Opt. Soc. Am. 55, 457 (1965).
- 3. W. T. Cathey, Jr., J. Opt. Soc. Am. 56, 1167 (1966).
- 4. J. C. Urbach and R. W. Meier, Proc. S.P.I.E. Seminar on Holography 15, 55 (1968).
- J. C. Urbach and R. W. Meier, Appl. Opt. 8, 2269 (1969).
- 6. J. H. Altman, Appl. Opt. 5, 1689 (1966).
- H. Kogelnik, Proc. Symposium on Modern Optics, Jerome Fox, Ed., Polytechnic Press, Brooklyn, N. Y., 1967.
- 8. H. Hannes, Optik 26, 363 (1967).
- 9. P. F. Mueller, J. Opt. Soc. Am. 57, 1419A (1967).
- 10. V. Russo and S. Sottini, Appl. Opt. 7, 202 (1968).
- 11. L. F. Collins, Appl. Opt. 7, 1236 (1968).
- 12. H. M. Smith, J. Opt. Soc. Am. 58, 533 (1968).
- 13. Von F. Bestenreiner and R. Deml, *Optik* **28**, 263 (1968).
- 14. R. L. Lamberts, J. Opt. Soc. Am. 59, 502A (1969).
- 15. H. M. Smith, J. Opt. Soc. Am. 58. 1492 (1968).
- K. S. Pennington and J. S. Harper, J. Opt. Soc. Am. 59, 481A (1969).
- 17. J. Upatnieks and C. D. Leonard, J. Opt. Soc. Am. 59, 481A (1969).
- R. L. Lamberts, C. N. Kurtz and C. D. Edgett, J. Opt. Soc. Am. 59, 1544A (1969).
- 19. L. H. Lin, Appl. Opt. 8, 963 (1969).
- R. A. Baugh, High-Efficiency Volume Holography, Ph.D. Thesis, Stanford University, 1969.
- 21. J. Upatnieks and C. D. Leonard, J. Opt. Soc. Am., (to be published).
- 22. Lord Rayleigh, *Philosophical Magazine* X, 73 (1880). (Also Scientific Papers, Vol. I, 491.)
- 23. J. W. Goodman, Introduction to Fourier Optics, Mc-Graw-Hill Book Co., Inc., San Francisco, Calif., 1968, p. 69.
- 24. E. Janke and F. Edme, *Tables of Functions*, Dover Publications Inc., New York, 1945.
- O. Bryngdahl and A. W. Lohmann, J. Opt. Soc. Am. 58, 141 (1968).
- 26. The use of Kodak SH-5 hardener before development, in conjunction with the cupric bleach EB-2, was reported by Pennington and Harper at the Spring 1969 Meeting of the Optical Society of America. We choose to use Kodak SH-1 hardener after fixing because hardening before development retarded both the overall speed of development and development in depth.
- 27. J. Upatnieks and C. D. Leonard, Appl. Opt. 8, 85 (1969).

Received December 12, 1969